LETTERS
PUBLISHED ONLINE: 11 AUGUST 2013 | DOI: 10.1038/NPHYS2711

nature physics

Distribution of entropy production in a single-electron box

J. V. Koski[1]*, T. Sagawa[2], O-P. Saira[1,3], Y. Yoon[1], A. Kutvonen[4], P. Solinas[1,4], M. Möttönen[1,5], T. Ala-Nissila[4,6] and J. P. Pekola[1]

Recently, the fundamental laws of thermodynamics have been reconsidered for small systems. The discovery of the fluctuation relations[1–5] has spurred theoretical[6–13] and experimental[14–25] studies. The concept of entropy production has been extended to the microscopic level by considering stochastic trajectories of a system coupled to a heat bath. However, this has not been studied experimentally if there are multiple thermal baths present. Here, we measure, with high precision, the distributions of microscopic entropy production in a single-electron box consisting of two islands with a tunnel junction. The islands are coupled to separate heat baths at different temperatures, maintaining a steady thermal non-equilibrium. We demonstrate that stochastic entropy production[8,10–12,17,20,25,26] from trajectories of electronic transitions is related to thermodynamic entropy production from dissipated heat in the respective thermal baths. We verify experimentally that the fluctuation relations for both definitions are satisfied. Our results reveal the subtlety of irreversible entropy production in non-equilibrium.

The second law of thermodynamics states that, on average, total entropy production is either zero or positive, the latter of which is a hallmark of irreversible processes. However, the so-called integral fluctuation theorem (IFT) reveals that negative entropy production is possible for an individual stochastic trajectory of the system. In systems that are not coupled to a thermal bath[17,20], the stochastic entropy production and work seem to have no obvious connection to their thermodynamic counterparts. The situation is further complicated by the fact that stochastic trajectories actually depend on the scale of observation. If one only accesses mesoscopic degrees of freedom, one observes coarse-grained trajectories of mesoscopic states. The corresponding entropy production then differs from that without coarse-graining. Recent experiments[25] with a driven colloidal particle in a bath of fluid have shown that coarse-graining of the slow background degrees of freedom may actually lead to a modification of the fluctuation relations. An important question that remains is what happens to a small system coupled to more than just one heat bath when the temperatures of the baths are not equal. Such a system goes naturally to a non-equilibrium state, but the dissipated heat of the baths can still be physically defined. To this end, we consider here the case of a two-level system coupled to two such thermal baths. We measure the distributions of entropy production at different levels of description, and clarify the connection between the stochastic entropy production and that of the heat baths.

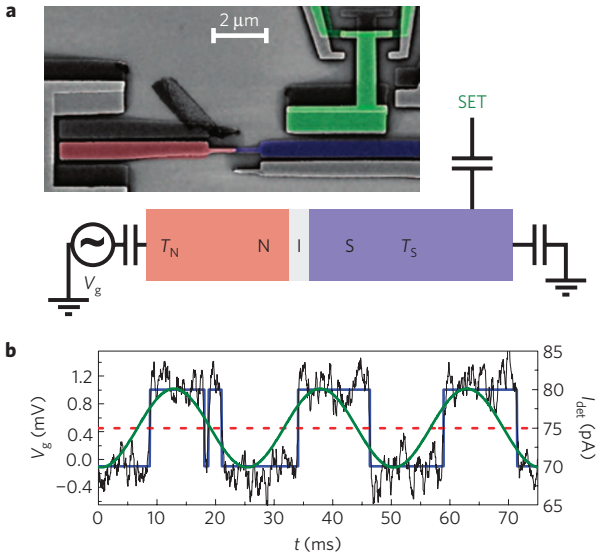

Figure 1 | Measurement set-up. a, Sketch of the measured system together with a scanning electron micrograph of a typical sample. The colours on the micrograph indicate the correspondingly coloured circuit elements in the sketch. **b**, Example trace of the measured detector signal under a sinusoidal protocol for the drive V_g, plotted in green. This trace covers three realizations of the forward protocol (V_g from −0.1 to 1 mV), and three realizations of the backward protocol (V_g from 1 to −0.1 mV). The SET current I_{det}, plotted in black, indicates the charge state of the box. The output of the threshold detection is shown in solid blue, with the threshold level as indicated by the dashed red line.

A single-electron box (SEB) at low temperatures is an excellent test bench for thermodynamics in small systems[24,27,28]. The SEB employed here is shown in Fig. 1a. The electrons in the normal-metal copper island (N) can tunnel to the superconducting Al island (S) through the aluminium oxide insulator (I). We denote by n the integer net number of electrons tunnelled from S to N relative to charge neutrality. As we can monitor the charge state n with a nearby single-electron transistor

[1]Low Temperature Laboratory (OVLL), Aalto University, POB 13500, FI-00076 AALTO, Finland, [2]Department of Basic Science, The University of Tokyo, Komaba 3-8-1, Meguro-ku, Tokyo 153-8902, Japan, [3]Kavli Institute of Nanoscience, Delft University of Technology, PO Box 5046, 2600 GA Delft, The Netherlands, [4]COMP Centre of Excellence, Department of Applied Physics, Aalto University School of Science, PO Box 11000, FI-00076 Aalto, Espoo, Finland, [5]QCD Labs, COMP Centre of Excellence, Department of Applied Physics, Aalto University School of Science, PO Box 13500, FI-00076 Aalto, Espoo, Finland, [6]Department of Physics, Brown University, Providence, Rhode Island 02912-1843, USA. *e-mail: jonne.koski@aalto.fi

(SET) shown in Fig. 1a, we take our classical system degree of freedom to be n.

The device in Fig. 1a can be represented with a classical electric circuit, in which the energy stored in the capacitors and the voltage sources is given by[27,29,30]

$$H(n_g,n)=E_C(n-n_g)^2-e^2n_g^2/(2C_g) \quad (1)$$

where E_C is the characteristic charging energy, C_g is the gate capacitance, $n_g=C_gV_g/e$ is the gate charge in units of the elementary charge e, and V_g is the gate voltage that drives the system externally. Equation (1) gives the internal energy of the system. In an instantaneous single-electron tunnelling event from $n=k$ to $n=k+1$, the drive parameters stay constant and hence the work done to the system vanishes. Thus the first law of thermodynamics states that the generated heat is given by

$$Q_k=H(n_g,k)-H(n_g,k+1)=E_C[2(n_g-k)-1] \quad (2)$$

It has been recently demonstrated that when the SEB is in thermal equilibrium and the transition rates obey the detailed balance condition, the Jarzynski Equality $\langle e^{-\beta W}\rangle=e^{-\beta\Delta F}$, relating the work done in the system W at inverse temperature $\beta=1/k_BT$ to its free energy change ΔF, can be verified both theoretically[27,28,30] and experimentally[24] to a high degree of accuracy. In the present work, however, the two environments consisting of the excitations in the normal metal and the superconductor are at different temperatures $T_N=1/(k_B\beta_N)$ and $T_S=1/(k_B\beta_S)$, respectively, and hence the Jarzynski Equality cannot be applied. Nevertheless, we expect that our system obeys the IFT[8],

$$\langle e^{-\Delta s_{tot}}\rangle=1 \quad (3)$$

for the total entropy production $\Delta s_{tot}=\Delta s+\Delta s_m$ given in terms of the increase of the system entropy $\Delta s=\ln\{P[n(t_f)]/P[n(0)]\}$ and the medium entropy production Δs_m. Here, $P[n(t)]$ is the directly measurable probability of the system to be in state n at time instant t given the initial condition and the drive $n_g(t)$.

As each heat bath is described by a thermal distribution, the total thermodynamic entropy production in the medium is given by

$$\Delta s_m^{th}=\beta_NQ_N+\beta_SQ_S$$

where Q_N and Q_S are the heat dissipated along the trajectory in the normal metal and in the superconductor, respectively. We can measure the total dissipated heat $Q=Q_N+Q_S$ directly by monitoring $n(t)$ with the SET and using equation (2). The only essential assumption here is that the tunnelling is elastic because the parameters of the Hamiltonian equation (1) can be measured independently. Heat is dissipated on N and S whenever n changes. For instance, in a transition $n{:}k\rightarrow k+1$ an electron tunnels from S to N. As illustrated in Fig. 2a, $-Q_S$ equals the energy carried by the electron, whereas $Q_N=-Q_S+Q$ equals the sum of the electron energy and the energy it gains according to equation (2). We can further obtain the conditional probability of Q_S on Q by some additional assumptions (for technical details, see Supplementary Information) and hence the probability distribution of Δs_m^{th}.

We can take a different approach by eliminating the dependence on Q_S in entropy production by averaging. Consider a single transition $n{:}k\rightarrow k\pm1$. For this, we define a coarse-grained entropy production in the medium Δs_m^{cc} as

$$e^{-\Delta s_m^{cc}(Q)}=\langle e^{-\Delta s_m^{th}(Q_S,Q)}\rangle_Q \quad (4)$$

where $\langle\cdots\rangle_Q$ denotes an average over the heat dissipated in Q_S for a fixed Q. It is shown in the Supplementary Information that this

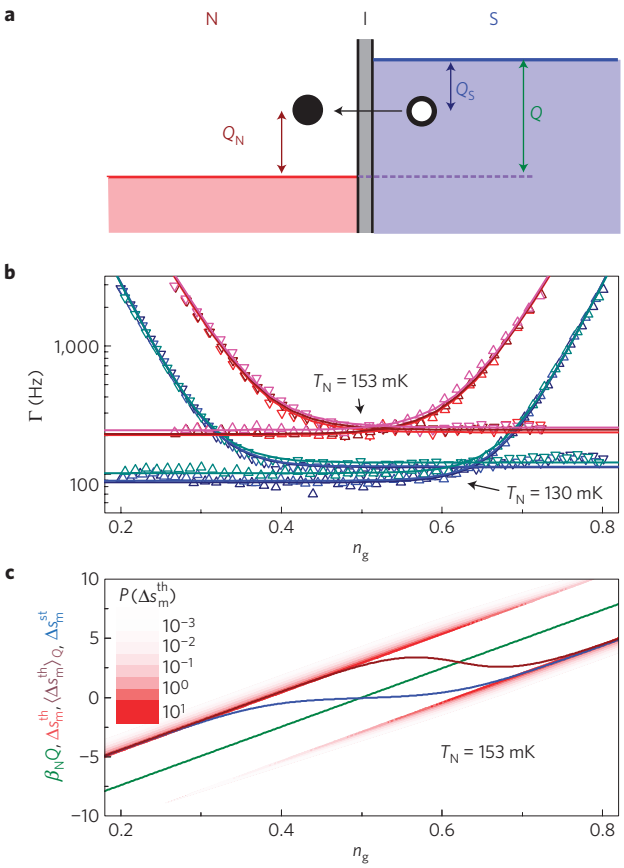

Figure 2 | Evaluation of entropy production. a, Energy diagram of a transition $0\rightarrow1$, where an electron tunnels from S to N. The event removes an energy $-Q_S$ from S with respect to its Fermi level and similarly adds Q_N to N. Δs_m^{th} depends on both Q_N and Q_S, whereas the total dissipated heat Q is always determined by the control parameter n_g. The energy gap in the superconductor density of states is not shown for simplicity. **b**, The tunnelling rates $\Gamma_{0\rightarrow1}$ (triangles pointing up) and $\Gamma_{1\rightarrow0}$ (triangles pointing down) for measurements 1–3 (dark blue, light blue and green symbols) and 8–10 (dark red, light red and pink symbols) with their corresponding fits (solid lines; for parameters see Table 1). **c**, Entropy produced by the transition $0\rightarrow1$ at 153 mK as a function of n_g at the time instant of the transition. Probability density of Δs_m^{th} along the y axis is shown in red, $\langle\Delta s_m^{th}\rangle_Q$ is shown in brown, the Δs_m^{st} extracted from **b** is shown in blue, and β_NQ is shown in green.

definition of entropy coincides with stochastic entropy production in the medium[8,13], which is defined as

$$\Delta s_m^{st}=\sum_j\ln\left[\frac{\Gamma_{n_-\rightarrow n_+}(t_j)}{\Gamma_{n_+\rightarrow n_-}(t_j)}\right]=\sum_j\Delta s_m^{cc}(Q_j)$$

where the system is taken to make transitions at time instants t_j from the state n_- to the state n_+, and $\Gamma_{n_-\rightarrow n_+}(t_j)$ and $\Gamma_{n_+\rightarrow n_-}(t_j)$ are the corresponding forward and backward transition rates, and Q_j is the total dissipated heat at that time instant. This derivation provides a physical interpretation for Δs_m^{st}, and by further noting that equation (4) implies $\langle\Delta s_m^{th}\rangle_Q\geq\Delta s_m^{cc}(Q)$, we may conclude that

$$\langle\Delta s_m^{th}\rangle\geq\langle\Delta s_m^{st}\rangle$$

Note that, by introducing transition rates, we have implicitly assumed that the system is Markovian, a fact that can be experimentally verified in our set-up.

Table 1 | Measurement parameters and obtained averages for work and entropy production.

Meas.	f (Hz)	T_N (mK)	n_0	$T_{S,0}$ (mK)	$T_{S,1}$ (mK)	$\langle e^{-\beta_N \bar{W}} \rangle$	$\langle e^{-\Delta s^{st}_{tot}} \rangle$	$\langle e^{-\Delta s^{th}_{tot}} \rangle$
1	20	130	0.526	174	177	93	1.085	1.063
2	40	130	0.516	174	177	129	1.064	1.053
3	80	130	0.507	176	178	180	1.074	1.083
4	20	142	0.513	179	181	20	1.064	1.030
5	40	142	0.509	179	181	30	1.054	1.047
6	80	142	0.505	180	181	45	1.096	1.100
7	120	141	0.504	181	182	68	1.241	1.324
8	40	153	0.502	184	184	11	1.095	1.058
9	80	153	0.503	184	185	15	1.140	1.139
10	120	153	0.502	185	186	20	1.301	1.370

$T_{S,0/1}$ is the superconductor S temperature matching the state $n = 0/1$, and $\bar{W} = W - \Delta F$.

By extracting the entropy production from each detector trace, we can experimentally obtain the probability distributions $P_{\rightleftarrows}(\Delta s^{th}_{tot})$ and $P_{\rightleftarrows}(\Delta s^{st}_{tot})$ of $\Delta s^{th}_{tot} = \Delta s + \Delta s^{th}_{m}$ and $\Delta s^{st}_{tot} = \Delta s + \Delta s^{st}_{m}$, respectively, and hence access the IFT of equation (3), which should be satisfied by all the distributions. Here, $P_{\rightarrow}$ is the distribution for a forward driving protocol $n_{g,\rightarrow}(t)$ and $P_{\leftarrow}$ corresponds to the backward protocol $n_{g,\leftarrow}(t) = n_{g,\rightarrow}(t_f - t)$. In addition, we expect our system to satisfy the so-called detailed fluctuation relations[5,13] (DFR)

$$P_{\rightleftarrows}(\Delta s^{st}_{tot})/P_{\rightleftarrows}(-\Delta s^{st}_{tot}) = e^{\Delta s^{st}_{tot}}$$
$$P_{\rightleftarrows}(\Delta s^{th}_{tot})/P_{\rightleftarrows}(-\Delta s^{th}_{tot}) = e^{\Delta s^{th}_{tot}} \quad (5)$$

In our experiments, we drive the system with the gate charge $n_g(t) = n_0 - A\cos(\pi f t)$, where $n_0 \approx A \approx 0.5$. Figure 1b shows the applied drive and an example trace of the detector current. Clearly, two discrete current levels corresponding to the charge states $n = 0$ and $n = 1$ are observable. Owing to the low bath temperatures, 130–160 mK, the relatively high charging energy $E_C \approx 162\,\mu\text{eV} = 1.88\,\text{K} \times k_B$, and low driving frequencies $f \leq 120$ Hz, the system essentially always finds the minimum-energy state at the extrema of the drive. Thus we partition the continuous measurement into legs of forward and backward protocols, for which the charge state and gate charge change from 0 to 1 and 1 to 0, respectively. Conversion of the current trace from such a leg using threshold detection yields a realization for a system trajectory $n(t)$, an ensemble of which is used to obtain the desired distributions. Moreover, the system entropy change Δs in equation (3) vanishes, and we thus need only to obtain Δs_m to assess the fluctuation relations.

Figure 2c shows the estimated Δs^{th}_{m} conditional probability distribution and Δs^{st}_{m} as functions of the drive n_g. To obtain Δs^{st}_{m}, the tunnelling rates $\Gamma_{i\rightarrow j}(n_g)$, shown in Fig. 2b, are measured and fitted by a standard sequential tunnelling model, see Supplementary Information for details. For $n_g \approx 0.4$–0.6, the tunnelling probability is primarily determined by the thermal excitations of the overheated superconductor and not by n_g. This leads to a nearly vanishing Δs^{st}_{m}, whereas the average of Δs^{th}_{m} remains positive as a sign of heat flow from hot S to cold N.

Table 1 presents a collection of measurement parameters as well as exponential averages for entropy production. Figures 3 and 4 show the experimentally obtained distributions for work and entropy production together with respective theoretical predictions for various T_N and f. As expected, the work distributions in Fig. 3a do not satisfy Jarzynski Equality. For comparison, the case $T_S = T_N$, where Jarzynski Equality is valid, is shown by the dashed lines. The difference between T_N and T_S decreases with increasing T_N, and hence the difference between data and the dashed lines decreases

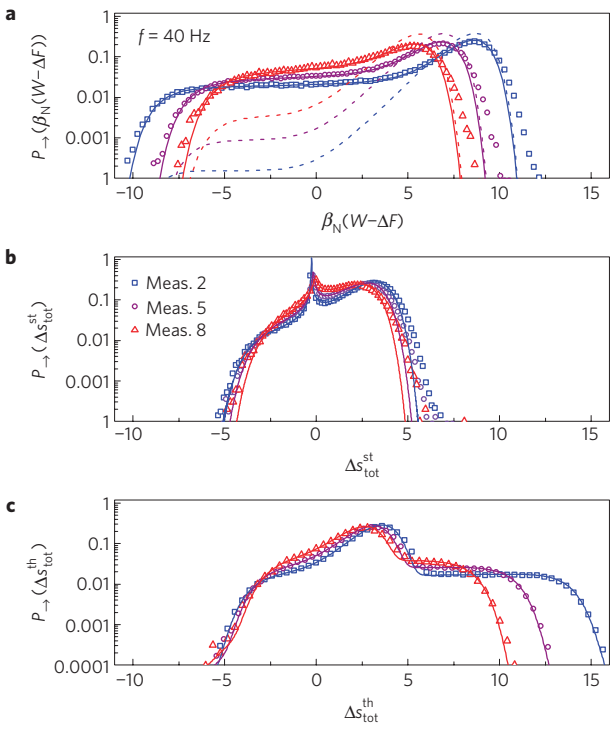

Figure 3 | Distributions of entropy production at different temperatures. **a**, $\beta_N(W - \Delta F)$ distributions for a 40 Hz forward protocol at different bath temperatures. The symbols show measured values (key in **b** applies to all panels), solid lines are numerical expectations (all panels), and dashed lines demonstrate what the distribution would be for $T_S = T_N$, such that Jarzynski Equality would be satisfied. **b**, Corresponding Δs^{st}_{tot} distributions. **c**, Δs^{th}_{tot} distributions for single jump trajectories.

as well. Conversely, all the entropy distributions in Figs 3b,c and 4, obtained from the same trajectories as the work distributions, satisfy the IFT within the experimental error. As it is relatively common that the transition $0 \rightarrow 1$ or $1 \rightarrow 0$ occurs when $n_g \approx 0.4$–0.6, one observes peaks in the Δs^{st}_{tot} distributions (Figs 3b and 4a,b) in the vicinity of zero, whereas the Δs^{th}_{tot} distributions (Figs 3c and 4c) exhibit a tail for positive Δs^{th}_{tot}, as indicated by Fig. 2c.

Figure 5a,b show the DFR for Δs^{st}_{tot} and Δs^{th}_{tot}, respectively. The Δs^{st}_{tot} distributions for forward and backward protocols, shown in Fig. 4b, are overlapping, apart from the positions of the peaks near vanishing Δs^{st}_{tot}. The offset of the peaks is explained by different superconductor temperatures (Table 1) for different tunnelling directions, leading to $\Gamma_{0\rightarrow 1}(n_g = 0.5) < \Gamma_{1\rightarrow 0}(n_g = 0.5)$. For the

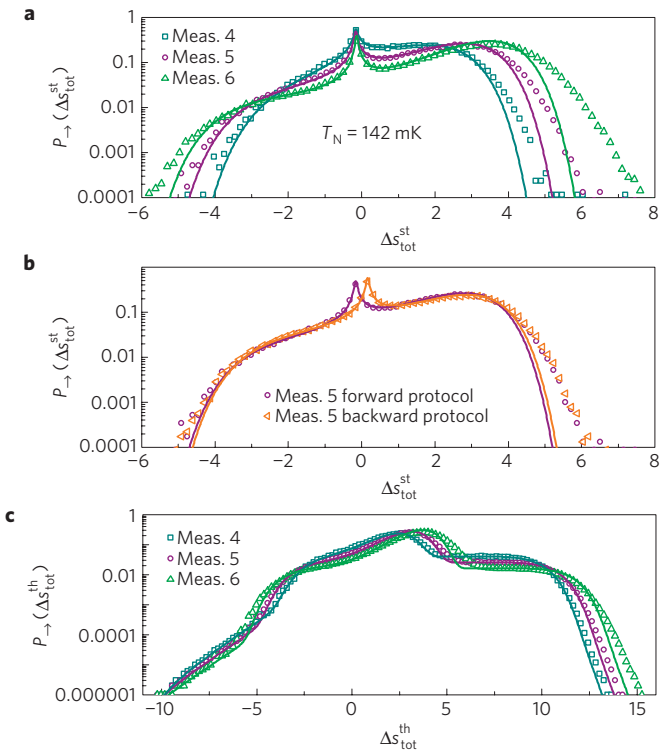

Figure 4 | Distributions of entropy production at different frequencies. **a**, Δs^{st}_{tot} distributions obtained at $T_N = 142$ mK with different drive frequencies. **b**, Distributions of an individual measurement for forward and backward protocols. **c**, Corresponding Δs^{th}_{tot} distributions for single jump trajectories.

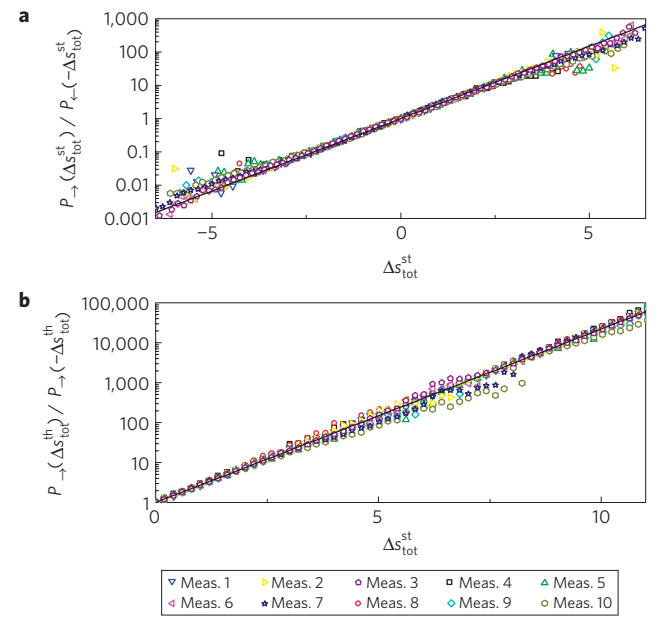

Figure 5 | Test of the DFR. **a**, DFR for Δs^{st}_{tot}. Despite the asymmetry of forward and backward protocols due to detector back-action, the relation is satisfied. **b**, DFR for Δs^{th}_{tot} of the forward protocol. In both **a** and **b**, the expected dependence given by equation (5) is shown as a solid black line.

$n{:}0 \rightarrow 1$ event, this corresponds to negative entropy production, whereas positive production is observed for $n{:}1 \rightarrow 0$. Different temperatures for different tunnelling directions can be justified by the difference in the observed tunnelling rates in Fig. 2b. The SET current is higher for $n = 1$ than for $n = 0$ (Fig. 1c), inducing a higher excess heating power for the superconductor at $n = 1$. However, even with these offsets in the Δs^{st}_{tot} distributions, they do obey the DFR.

Our measured distributions satisfy the IFT and DFR, verifying the fluctuation relations in thermal non-equilibrium. The fluctuation relations can be used to determine thermodynamic quantities such as free energy. Moreover, these relations apply even beyond the linear response regime, whereas the conventional fluctuation-dissipation theorem, widely used for instance in condensed matter physics, is a result of linear response theory with limited applicability to non-equilibrium processes.

Methods

The sample fabrication methods (see Supplementary Information for details) are similar to those in ref. 24, but the design is different such that the S side of the junction does not overlap with the normal conductor to intentionally weaken the relaxation of energy in S (ref. 31). Moreover, the main results in ref. 24 were extracted from measurements at a temperature of 220 mK, whereas the present measurements are conducted at 140 mK. Lower temperature further weakens the relaxation significantly[31], leading to a steady elevated temperature in S.

The tunnelling rates are solved by comparing the measured data to the outcome from the master equation, see Supplementary Information for details. The rates from the standard sequential tunnelling model are in agreement with the experimentally obtained data. Utilizing the model as a fit yields the charging energy, the tunnelling resistance of the junction $R_T \approx 1.7\,\mathrm{M\Omega}$, and the excitation gap of the superconductor $\Delta \approx 224\,\mu\mathrm{eV}$. T_N is assumed to be the temperature of the cryostat, whereas T_S is obtained for each measurement from the fit as listed in Table 1.

Received 25 March 2013; accepted 2 July 2013; published online 11 August 2013

References

1. Evans, D. J., Cohen, E. G. D. & Morriss, G. P. Probability of second law violations in shearing steady states. *Phys. Rev. Lett.* **71,** 2401–2404 (1993).
2. Gallavotti, G. & Cohen, E. G. D. Dynamical ensembles in nonequilibrium statistical mechanics. *Phys. Rev. Lett.* **74,** 2694–2697 (1995).
3. Jarzynski, C. Nonequilibrium equality for free energy differences. *Phys. Rev. Lett.* **78,** 2690–2693 (1997).
4. Kurchan, J. Fluctuation theorem for stochastic dynamics. *J. Phys. A.* **31,** 3719–3729 (1998).
5. Crooks, G. E. Entropy production fluctuation theorem and the nonequilibrium work relation for free energy differences. *Phys. Rev. E* **60,** 2721–2726 (1999).
6. Jarzynski, C. Hamiltonian derivation of a detailed fluctuation theorem. *J. Stat. Phys.* **98,** 77–102 (2000).
7. Hatano, T. & Sasa, S. I. Steady-state thermodynamics of Langevin systems. *Phys. Rev. Lett.* **86,** 3463–3466 (2001).
8. Seifert, U. Entropy production along a stochastic trajectory and an integral fluctuation theorem. *Phys. Rev. Lett.* **95,** 040602 (2005).
9. Sagawa, T. & Ueda, M. Generalized Jarzynski equality under nonequilibrium feedback control. *Phys. Rev. Lett.* **104,** 090602 (2010).
10. Kawai, R., Parrondo, J. M. R. & Van den Broeck, C. Dissipation: The phase-space perspective. *Phys. Rev. Lett.* **98,** 080602 (2007).
11. Gomez-Marin, A., Parrondo, J. M. R. & Van den Broeck, C. Lower bounds on dissipation upon coarse graining. *Phys. Rev. E* **78,** 011107 (2008).
12. Esposito, M. Stochastic thermodynamics under coarse graining. *Phys. Rev. E* **85,** 041125 (2012).
13. Seifert, U. Stochastic thermodynamics, fluctuation theorems and molecular machines. *Rep. Prog. Phys.* **75,** 126001 (2012).
14. Wang, G. M., Sevick, E. M., Mittag, E., Searles, D. J. & Evans, D. J. Experimental demonstration of violations of the second law of thermodynamics for small systems and short time scales. *Phys. Rev. Lett.* **89,** 050601 (2002).
15. Liphardt, J., Dumont, S., Smith, S. B., Tinoco, I. Jr. & Bustamante, C. Equilibrium information from nonequilibrium measurements in an experimental test of Jarzynski's equality. *Science* **296,** 1832–1835 (2002).
16. Trepagnier, E. H. *et al.* Experimental test of Hatano and Sasa's nonequilibrium steady-state equality. *Proc. Natl Acad. Sci. USA* **101,** 15038–15041 (2004).
17. Schuler, S., Speck, T., Tietz, C., Wrachtrup, J. & Seifert, U. Experimental test of the fluctuation theorem for a driven two-level system with time-dependent rates. *Phys. Rev. Lett.* **94,** 180602 (2005).
18. Collin, D. *et al.* Verification of the Crooks fluctuation theorem and recovery of RNA folding free energies. *Nature* **437,** 231–234 (2005).
19. Blickle, V., Speck, T., Helden, L., Seifert, U. & Bechinger, C. Thermodynamics of a colloidal particle in a time-dependent nonharmonic potential. *Phys. Rev. Lett.* **96,** 070603 (2006).

20. Tietz, C., Schuler, S., Speck, T., Seifert, U. & Wrachtrup, J. Measurement of stochastic entropy production. *Phys. Rev. Lett.* **97,** 050602 (2006).
21. Speck, T., Blickle, V., Bechinge, C. & Seifert, U. Distribution of entropy production for a colloidal particle in a nonequilibrium steady state. *Europhys. Lett.* **79,** 30002 (2007).
22. Nakamura, S. *et al.* Nonequilibrium fluctuation relations in a quantum coherent conductor. *Phys. Rev. Lett.* **104,** 080602 (2010).
23. Toyabe, S., Sagawa, T., Ueda, M., Muneyuki, E. & Sano, M. Experimental demonstration of information-to-energy conversion and validation of the generalized Jarzynski equality. *Nature Phys.* **6,** 988–992 (2010).
24. Saira, O-P. *et al.* Test of the Jarzynski and Crooks fluctuation relations in an electronic system. *Phys. Rev. Lett.* **109,** 180601 (2012).
25. Mehl, J. *et al.* Role of hidden slow degrees of freedom in the fluctuation theorem. *Phys. Rev. Lett.* **108,** 220601 (2012).
26. Kawaguchi, K. & Nakayama, Y. Fluctuation theorem for hidden entropy production. Preprint at http://arxiv.org/abs/1209.6333 (2012).
27. Averin, D. V. & Pekola, J. P. Statistics of the dissipated energy in driven single-electron transitions. *Europhys. Lett.* **96,** 67004 (2011).
28. Pekola, J. P., Kutvonen, A. & Ala-Nissila, T. Dissipated work and fluctuation relations for non-equilibrium single-electron transitions. *J. Stat. Mech.* P02033 (2013).
29. Averin, D. V. & Likharev, K. K. Coulomb blockade of single-electron tunneling, and coherent oscillations in small tunnel-junctions. *J. Low Temp. Phys.* **62,** 345–373 (1986).
30. Pekola, J. P. & Saira, O-P. Work, free energy and dissipation in voltage driven single-electron transitions. *J. Low Temp. Phys.* **169,** 70–76 (2012).
31. Maisi, V. F. *et al.* Single quasiparticle excitation dynamics on a superconducting island. Preprint at http://arxiv.org/abs/1212.2755 (2013).

Acknowledgements

This work has been supported in part by the Academy of Finland though its LTQ (project no. 250280) and COMP (project no. 251748) CoE grants, the European Union Seventh Framework Programme INFERNOS (FP7/2007–2013) under grant agreement no. 308850, the Research Foundation of Helsinki University of Technology, and the Väisälä Foundation. We acknowledge Micronova Nanofabrication Centre of Aalto University for providing the processing facilities and technical support. We thank D. Averin, S. Gasparinetti, F. Hekking, K. Likharev, V. Maisi and M. Meschke for useful discussions.

Author contributions

J.V.K., O-P.S., Y.Y. and J.P.P. conceived and designed the experiments; J.V.K., O-P.S. and Y.Y. performed the experiments; J.V.K. and M.M. analysed the data. All authors contributed with materials/analysis tools; J.V.K., T.S., M.M., T.A-N. and J.P.P. wrote the paper.

Additional information

Supplementary information is available in the online version of the paper. Reprints and permissions information is available online at www.nature.com/reprints. Correspondence and requests for materials should be addressed to J.V.K.

Competing financial interests

The authors declare no competing financial interests.